



Contents lists available at ScienceDirect

Solid State Electronics

journal homepage: www.elsevier.com/locate/sse

Resistive switching characteristics of solution-processed Al–Zn–Sn–O films annealed by microwave irradiation

Tae-Wan Kim, Il-Jin Baek, Won-Ju Cho*

Department of Electronic Materials Engineering, Kwangjuon University, 447-1, Wolgye-dong, Nowon-gu, Seoul 139-701, Republic of Korea

ARTICLE INFO

Keywords:

ReRAM
MWI
AZTO
Solution process
BRS
MLC

ABSTRACT

In this study, we employed microwave irradiation (MWI) at low temperature in the fabrication of solution-processed AlZnSnO (AZTO) resistive random access memory (ReRAM) devices with a structure of Ti/AZTO/Pt and compared the memory characteristics with the conventional thermal annealing (CTA) process. Typical bipolar resistance switching (BRS) behavior was observed in AZTO ReRAM devices treated with as-deposited (as-dep), CTA and MWI. In the low resistance state, the Ohmic conduction mechanism describes the dominant conduction of these devices. On the other hand, the trap-controlled space charge limited conduction (SCLC) mechanism predominates in the high resistance state. The AZTO ReRAM devices processed with MWI showed larger memory windows, uniform distribution of resistance state and operating voltage, stable DC durability ($> 10^3$ cycles) and stable retention characteristics ($> 10^4$ s). In addition, the AZTO ReRAM devices treated with MWI exhibited multistage storage characteristics by modulating the amplitude of the reset bias, and eight distinct resistance levels were obtained with stable retention capability.

1. Introduction

Recently, amorphous indium-gallium-zinc oxide (a-IGZO) thin film transistors (TFTs) are emerging as a new generation of active matrix backplane technology in high-performance liquid crystal displays (LCDs) and organic light-emitting diode (OLED) displays because a-IGZO is advantageous for large area electronic devices. These advantages include uniform deposition in a large area, optical transparency and a smooth surface. In addition, the a-IGZO TFTs exhibits a much higher electron mobility ($> 10 \text{ cm}^2/\text{V}\cdot\text{s}$) than the hydrogenated amorphous silicon (a-Si:H) TFTs, and has relatively low cost and high uniformity compared to conventional polycrystalline Si (poly-Si) TFTs [1–3]. Due to its excellent resistance switching characteristics in standard metal-insulator-metal (MIM) structures, the a-IGZO film has been studied as an active layer of resistive switching random access memory (ReRAM) devices. The a-IGZO layer has better mechanical durability than polycrystalline state, and is applicable to multi-level cells (MLC) for higher storage density due to the high ON/OFF resistance window [4,5].

Moreover, the a-IGZO ReRAM device can be easily integrated with the a-IGZO TFTs in the backplane of the emerging transparent flat panel display (FPD) for system-on-a-panel (SoP) applications [6]. However, indium (In) and gallium (Ga), which are rare elements on the earth, are becoming increasingly expensive and potentially scarce because of the

large demand for the manufacture of optoelectronic devices [7,8]. Alternatively, amorphous aluminum doped zinc tin oxide (a-AZTO) without In and Ga components has attracted considerable interest as a substitute for a-IGZO due to its low material cost [9,10]. Generally, amorphous oxide semiconductors are produced by vacuum processes such as rf magnetron sputtering or pulsed laser deposition, which require high manufacturing costs [11,12]. On the other hand, solution-based film-deposition processes such as spin-coating or ink-jet processes provide significant advantages including low cost, precise composition control and high throughput. However, compared to vacuum-processed films, solution-processed films exhibit inferior resistance switching (RS) characteristics due to the difficulty of defect control, such as dislocation, grain boundary, metal ions, oxygen vacancies, and organic impurities form organic precursors [13]. For this reason, the convention thermal annealing (CTA) process is predominantly employed to reduce the defects in solution-processed films [14]. However, due to the high temperatures, the CTA process is limited to use in the manufacture of devices based on transparent or flexible substrates such as glass, plastic or paper. As a result, plasma exposure, ultraviolet (UV) ozone treatment, high-energy electron beam irradiation and microwave irradiation (MWI) are considered as alternative CTA methods [15–19]. Among these processes, the MWI process is perceived as one of the most efficient and promising processes owing to the fast delivery and uniformity of energy, smooth surface, and improved reliability at low temperatures

* Corresponding author.

E-mail address: chowj@kw.ac.kr (W.-J. Cho).<http://dx.doi.org/10.1016/j.sse.2017.10.029>

0038-1101/ © 2017 Elsevier Ltd. All rights reserved.

of IGZO ReRAM devices [20]. Nevertheless, there are still few reports on the resistive switching of solution-processed AZTO film based ReRAMs. To the best of our knowledge, this is the first study to report the impact of MWI treatment on the AZTO ReRAMs. The MWI process can transfer energy directly to the target material by absorbing microwave energy over the entire volume of the target material. Moreover, it has several advantages such as low temperature, thermal uniformity, short processing time and selective heating of materials [19,20].

To verify the effect of MWI process, the electrical characteristics and memory characteristics of ReRAM devices fabricated by CTA process were compared. Furthermore, we evaluated the potential of system-on-a-panel (SoP) applications by studying the multilevel operation capacity and highly endurable cycling test.

2. Experimental method

To prepare the AZTO precursor solution, 0.1 M aluminum chloride (AlCl_3 , Sigma-Aldrich, 99.9%), zinc nitrate hydrate ($\text{Zn}(\text{NO}_3)_2 \cdot x\text{H}_2\text{O}$, Sigma-Aldrich, 99.9%), and tin chloride (SnCl_2 , Sigma-Aldrich, 99.9%) were dissolved in 20 mL of 2-methoxyethanol ($\text{CH}_3\text{OCH}_2\text{CH}_2\text{OH}$, 2ME) with $\text{Al}:\text{Zn}:\text{Sn} = 0.2:1:1$ composition ratio. This mixed solution was then stirred at 1500 rpm for 24 h. In order to obtain a homogeneous solution, monoethanolamine (MEA) and acetic acid were added into the solution under continuous stirring. The solution obtained was filtered using a $0.2\ \mu\text{m}$ inorganic membrane syringe filter (Whatman, UK). Heavily doped p-type (100) silicon substrates with 300-nm-thick thermal oxide layer were used to fabricate solution-processed AZTO ReRAM devices. A 10-nm-thick Ti layer and a 100-nm-thick Pt layer for bottom electrodes (BE) were sequentially deposited using an electron beam evaporator. Subsequently, the final AZTO solution ($\text{Al}:\text{Zn}:\text{Sn} = 0.2:1:1$) was spin coated on the BE at 6000 rpm for 30 s at room temperature, and the coated AZTO film was dried at 250°C for 30 min to evaporate the solvent. Post-deposition annealing was implemented using a microwave irradiation system with 1000 W for 15 min in the ambient air. For comparison, the CTA process was executed in a furnace at 400°C for 30 min in ambient N_2 . The thicknesses of as-deposited (as-dep), CTA-treated, and MWI-treated AZTO films were 95, 86, and 75 nm, respectively. Finally, the 100-nm-thick Ti top electrodes (TE) with a diameter of $200\ \mu\text{m}$ were formed by electron beam evaporation using a shadow mask.

Fig. 1 shows a cross-sectional schematic representation of fabricated solution-processed AZTO ReRAM devices of Ti/AZTO/Pt structure. The resistive switching behavior of the fabricated ReRAM devices was characterized using a two-probe measurement system with an Agilent 4156B precision semiconductor parameter analyzer in a dark box. The chemical bonding configurations of a-AZTO films were investigated using X-ray photoelectron spectroscopy (XPS).

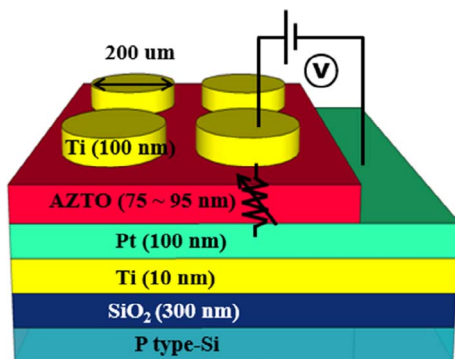


Fig. 1. Schematic representation of fabricated solution-processed AZTO ReRAM devices of Ti/AZTO/Pt structure.

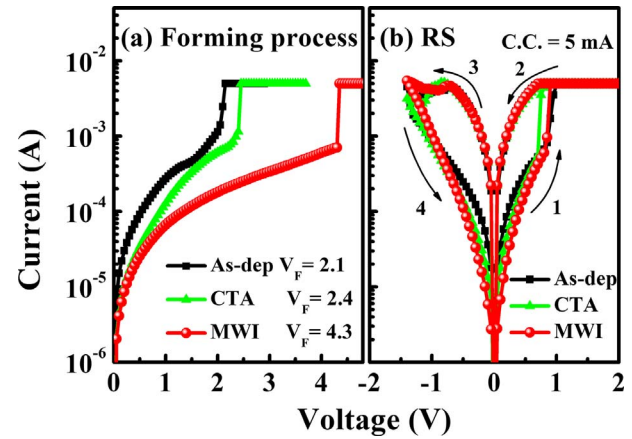


Fig. 2. (a) Forming process and (b) typical bipolar resistive switching behaviors of as-dep, CTA, and MWI-treated solution-processed AZTO ReRAMs.

3. Results and discussion

Fig. 2(a) shows the initial current–voltage (I – V) characteristics of as-dep, CTA-treated, and MWI-treated AZTO ReRAM devices measured using a DC-sweep mode with a current compliance of 5 mA. An external bias was applied to the TE, while the BE was electrically grounded. Initial resistive states were suddenly changed from a high resistance state (HRS) to a low resistance state (LRS), under the positive TE bias around 5 V, defined as forming process. The forming voltages of as-dep, CTA-treated, and MWI-treated AZTO ReRAM devices were 2.1 V, 2.4 V, and 4.3 V, respectively.

Fig. 2(b) shows the typical bipolar resistive switching (BRS) behaviors of as-dep, CTA-treated, and MWI-treated AZTO ReRAM devices. When a positive DC bias sweep is applied at zero, a steep increase in current is observed with a current compliance of 5 mA at approximately 1 V (arrow 1). At this point, the HRS changes to an LRS and is defined as a set process. When a negative bias is applied to the TE, an abrupt decrease in current is observed in the disconnected conductive path at approximately $-1\ \text{V}$. This behavior shows that the resistance has switched from LRS to HRS, defined as a reset process (arrow 3). The HRS is maintained from a negative bias to zero applied voltage (arrow 4). Therefore, stable BRS characteristics exist in the AZTO ReRAM device. When positive and negative voltages are applied to the TE, the marked arrows sweep from 1 to 4.

To further discuss the conduction mechanisms of the as-dep, CTA-treated and MWI-treated AZTO ReRAMs of the Ti/AZTO/Pt structure, the I – V curves are replotted into a log–log scale as shown in Fig. 3. As the slope of LRS is close to 1, corresponding to the Ohmic behavior, the conduction behavior is governed by Ohmic-like conduction [21]. On the other hand, the slope of the HRS is close to 1 in the low voltage range. However, at voltages higher than $\sim 0.1\ \text{V}$ the current begins to increase non-linearly. This implies that different conduction components likely dominate in this region. Precise curve fitting indicates that the set process follows a trap-controlled space-charge-limited conduction (SCLC) mechanism with shallow traps. The charge transport mechanisms of HRS can be described using three regimes, which are Ohmic-like behavior in region (1), trap-filled-limited (TFL) behavior in region (2), and Child's law with increasing voltage in region (3). In region (1), the injected carrier density is lower than the thermally generated carrier density and the conduction follows Ohm's law. With increasing V , the injected carriers become predominant and a trap-filled-limited current is observed in region (2). The transition voltage from the Ohmic to trap-filled-limited behavior is defined as V_{ON} . When all of the traps are filled with the injected carriers under the higher voltage, a sudden jump in current occurs at V_{TFL} and then the I – V behavior follows Child's law in region (3) [22]. Eventually, the AZTO film switches to the LRS at V_{SET} .

Download English Version:

<https://daneshyari.com/en/article/7150592>

Download Persian Version:

<https://daneshyari.com/article/7150592>

[Daneshyari.com](https://daneshyari.com)